Background modeling and simulation of the calibration source for the CRESST dark matter search experiment

S. Banik,[b,c,*] G. Angloher,[a] G. Benato,[d] A. Bento,[a,i] A. Bertolini,[a] R. Breier,[e]
C. Bucci,[d] J. Burkhart,[b] L. Canonica,[a,m] A. D'Addabbo,[d] S. Di Lorenzo,[a] L. Einfalt,[b,c]
A. Erb,[f,j] F. v. Feilitzsch,[f] S. Fichtinger,[b] D. Fuchs,[a] A. Garai,[a] V.M. Ghete,[b]
P. Gorla,[d] P.V. Guillaumon,[d] S. Gupta,[b] D. Hauff,[a] M. Ješkovský,[e] J. Jochum,[g]
M. Kaznacheeva,[f] A. Kinast,[f] H. Kluck,[b] H. Kraus,[h] S. Kuckuk,[g] A. Langenkämper,[a]
M. Mancuso,[a] L. Marini,[d,k] B. Mauri,[a] L. Meyer,[g] V. Mokina,[b] M. Olmi,[d] T. Ortmann,[f]
C. Pagliarone,[d,l] L. Pattavina,[d,f] F. Petricca,[a] W. Potzel,[f] P. Povinec,[e] F. Pröbst,[a]
F. Pucci,[a] F. Reindl,[b,c] J. Rothe,[f] K. Schäffner,[a] J. Schieck,[b,c] S. Schönert,[f]
C. Schwertner,[b,c] M. Stahlberg,[a] L. Stodolsky,[a] C. Strandhagen,[g] R. Strauss,[f]
I. Usherov,[g] F. Wagner,[b] M. Willers[f] and V. Zema[a] (CRESST collaboration)

[a]*Max-Planck-Institut für Physik, D-80805 München, Germany*

[b]*Institut für Hochenergiephysik der Österreichischen Akademie der Wissenschaften, A-1050 Wien, Austria*

[c]*Atominstitut, Technische Universität Wien, A-1020 Wien, Austria*

[d]*INFN, Laboratori Nazionali del Gran Sasso, I-67100 Assergi, Italy*

[e]*Comenius University, Faculty of Mathematics, Physics and Informatics, 84248 Bratislava, Slovakia*

[f]*Physik-Department, Technische Universität München, D-85747 Garching, Germany*

[g]*Eberhard-Karls-Universität Tübingen, D-72076 Tübingen, Germany*

[h]*Department of Physics, University of Oxford, Oxford OX1 3RH, United Kingdom*

[i]*also at: LIBPhys-UC, Departamento de Fisica, Universidade de Coimbra, P3004 516 Coimbra, Portugal*

[j]*also at: Walther-Meißner-Institut für Tieftemperaturforschung, D-85748 Garching, Germany*

[k]*also at: GSSI-Gran Sasso Science Institute, I-67100 L'Aquila, Italy*

[l]*also at: Dipartimento di Ingegneria Civile e Meccanica, Università degli Studi di Cassino e del Lazio Meridionale, I-03043 Cassino, Italy*

[m]*present address: INFN, Sezione di Milano LASA, I-20054 Segrate, Milano, Italy*

E-mail: samir.banik@oeaw.ac.at

*Speaker

The Cryogenic Rare Event Search with Superconducting Thermometers (CRESST) experiment employs scintillating crystals at extremely low temperatures ($\mathcal{O}(10\,\text{mK})$) to search for nuclear recoils from hypothetical dark matter (DM) particles. CRESST has achieved thresholds below 100 eV with a wide range of target materials including $CaWO_4$, $LiAlO_2$, Al_2O_3, and Si. However, at these energies, the ability to discriminate between potential DM signals and electromagnetic background is insufficient. A detailed Geant4-based electromagnetic background model was developed for CRESST and is being continuously adapted to CRESST's current inventory of detector modules. We use a high-dimensional Bayesian likelihood fit of spectral templates to the measured spectrum to infer activities of various background sources. A template for the calibration source used to calculate the energy scale will be included in the likelihood fit. We present the status of CRESST's background model, and results from the simulation of the energy calibration. Our future plans of improving the background model are also discussed.

1. Introduction

The nature of dark matter (DM) is one of the greatest puzzling questions to be answered by modern physics. The Cryogenic Rare Event Search with Superconducting Thermometers (CRESST) is a direct-detection experiment focusing on the search for sub-GeV DM particles. It employs cryogenic detectors which are capable of measuring sub-keV nuclear recoils from DM via measurement of athermal phonons. CRESST uses as second channel the scintillation light to separate nuclear recoils from interactions with the atomic electrons. The experiment traditionally uses scintillating $CaWO_4$ as the main target material, and has been extending its inventory by including additional materials such as $LiAlO_2$, Al_2O_3, Si (non-scintillating) and diamond. A reliable background model is crucial for improving the current sensitivity of dark matter search with CRESST.

The first CRESST electromagnetic background model was introduced in 2009 [1]. The model fitted the prominent peaks in the measured CRESST data with Gaussian functions assuming a secular equilibrium (SE) within the decay chains of natural isotopes of uranium and thorium. In a recent research, we re-examined the SE assumption in a $CaWO_4$ crystal grown at Technische Universität München (TUM) [2], leading to the development of a revised background model. The updated model relaxes the SE assumption and adopts a high-dimensional Bayesian Likelihood fit [3]. To extend the model further, we will consider various other detector modules, and therefore new sources of backgrounds and impacts of new calibration sources on the measured data will be considered. In this proceeding, we describe the sources of backgrounds and their mitigation in Section 2, the CRESST background model in Section 3, investigation on the energy-scale-calibration source in Section 4, and conclude in Section 5.

## 2. Sources of backgrounds and mitigation

The sources of backgrounds for the dark matter search at CRESST include cosmic muons, ambient neutrons, ambient gamma radiation, cosmogenic activation, and internal contamination of the detector crystal and surrounding parts of the experiment, with the major contributions arising from the latter two. Cosmic muon impact is mitigated by the mountain above LNGS (a factor of $\sim 10^{-6}$ smaller flux), with plastic scintillator panels vetoing any residual muons, neutrons are effectively shielded by polyethylene [4], and the ambient gamma backgrounds are significantly reduced by lead and copper shieldings used in the experiment. The residual backgrounds causing energy depositions in the detector crystal are thoroughly modeled. Table 1 provides the major categories of backgrounds and various nuclides within these categories. A comprehensive account of all backgrounds in CRESST is provided in Ref. [1, 3].

3. CRESST background model

The background sources outlined in Section 2 are simulated using the Geant4-based tool "ImpCRESST" [1]. The simulation provides spectral templates (see Fig. 4 in Appendix A) describing the energy deposition for each background source. These templates are subsequently normalized using either a) Gaussian Fit Method (GFM), traditionally employed under the assumption of secular equilibrium within the decay chains [1], or b) Bayesian Likelihood Normalization Method

3

Table 1: Various categories and nuclides considered in the background model in CRESST.

Component	Nuclide
Internal Radiogenic (IR) of $CaWO_4$	^{238}U-, ^{235}U-, ^{232}Th- decay chains, ^{40}K
Internal Cosmogenic (IC) of $CaWO_4$	^{3}H, ^{179}Ta, ^{181}W
Near External Radiogenic (NER) by the detector holder	^{238}U-, ^{235}U-, ^{232}Th- decay chains, ^{40}K
Additional External Radiogenic (AER)	^{40}K, ^{208}Tl, ^{210}Pb, ^{212}Pb, ^{212}Bi, ^{214}Bi, ^{226}Ra, ^{228}Ra, ^{228}Ac, ^{234}Th
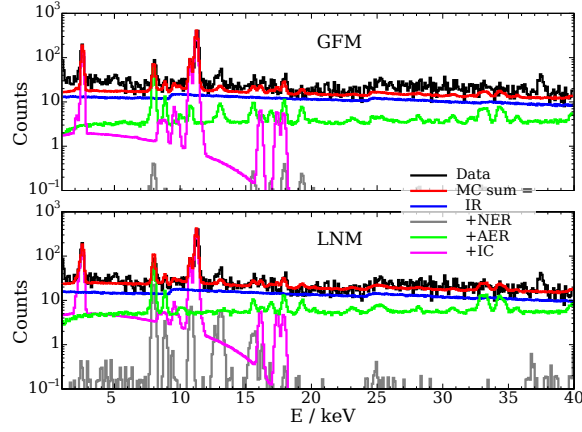
Figure 1: Decomposition of the modeled background, fitted via Gaussian Fit Method or LNM, to data into IR, NER, AER, and IC components [3].

(LNM) [3], a recent inclusion that relaxes the secular equilibrium assumption. The latter method has been demonstrated to provide a more precise description of the data. Figure 1 shows the normalized spectral templates from the two methods, where the data taken with TUM40 detector was used for the fits, resulting in a better background description below 10 keV.

4. Simulation of energy scale calibration

The ^{55}Fe source used for energy calibration in CRESST III is covered by a layer of glue to suppress the Auger electrons which would otherwise reach the crystal. A layer of gold is added on top of this structure to shield the detectors from possible scintillation light created in the glue. The source with this encapsulation is placed on a screw facing the target crystal and light detector of the module (see Fig. 5(a,b) in Appendix A). In the following, we discuss the impact of the source position with respect to phonon and light detector (Section 4.1), and the source encapsulation on the energy deposition spectrum (Section 4.2, 4.3).

4.1 Impact of source position on energy deposition in silicon

The source placement in the silicon module is assymetric with respect to the bulk and wafer detector (see Figure 5(c) in Appendix A), the solid angle subtended by the bulk detector's surface
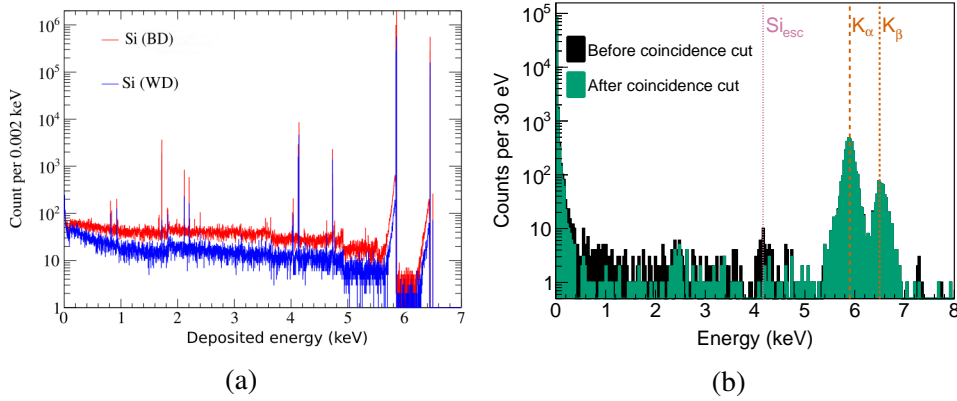
(a)   (b)

Figure 2: (a) Simulated spectra of energy depositions due to the ^{55}Fe source. (b) Measured spectra in the silicon wafer detector before and after selecting events coincident with the bulk detector [5].

facing the wafer detector is smaller compared to the same by the wafer detector surface. The simulated energy depsitions in the silicon target of bulk (BD) and wafer (WD) detectors due to the ^{55}Fe source, and the measured spectrum in the WD are shown in Fig. 2(a,b). After being fully absorbed in the crystals, the K$_\alpha$ (energy ~5.89 keV) and K$_\beta$ (~6.49 keV) X-rays from the source show the respective peaks in the distributions. The X-rays from the calibration source can also excite Si atoms in the BD or WD crystals, producing X-rays with an energy of 1.74 keV, which in turn can escape the respective crystals. The X-rays that escaped from the WD, when captured by the BD, produce a peak at 1.74 keV in the BD and an escape peak with the remaining energy of 4.16 keV in the BD; vice versa this is also true for the escaped X-rays from the BD. The X-ray and escape peaks in the BD and WD detectors are visible in the simulated spectrum (see Fig. 2(b)), however the 1.74 keV-peak in the WD is highly suppressed. This is due to the low solid angle subtended by the bulk surface ($\frac{1}{30}$ times the solid angle subtended by WD surface) resulting in fewer escaped X-rays from the BD that are reaching the WD. In the measured spectrum of the WD (see Fig. 2(b)), the X-ray that escapes from the detector are clearly visible as a peak at 4.16 keV, but no peak appears at 1.74 keV because little to no X-rays escape from the BD. This observation is in agreement with the simulation that predicts ~0.08 events at the 1.74 keV-peak of the WD.

4.2 Impact of source encapsulation on relative intensity of X-ray absorption peaks

The attenuation of X-rays in a material is energy dependent. This results in a non-uniform suppression of K$_\alpha$ and K$_\beta$ X-rays as they pass through the glue and gold layers around the ^{55}Fe source. The ratios of events between the two peaks in the presence and absence of encapsulation are found to be 3.56 and 6.43 respectively, indicating a stronger suppression of K$_\alpha$ X-rays compared to the K$_\beta$ X-rays when encapsulated by the glue and gold.

4.3 Impact of the encapsulation on the energy deposition spectrum in a sapphire module

A bump is observed around 140 eV in the simulated spectrum in the sapphire module, similar to a feature in the measured spectrum at a slightly higher energy of 180 eV. The comparison of simulated and measured spectra is shown in Fig. 3(a). The bump in the simulated spectrum is
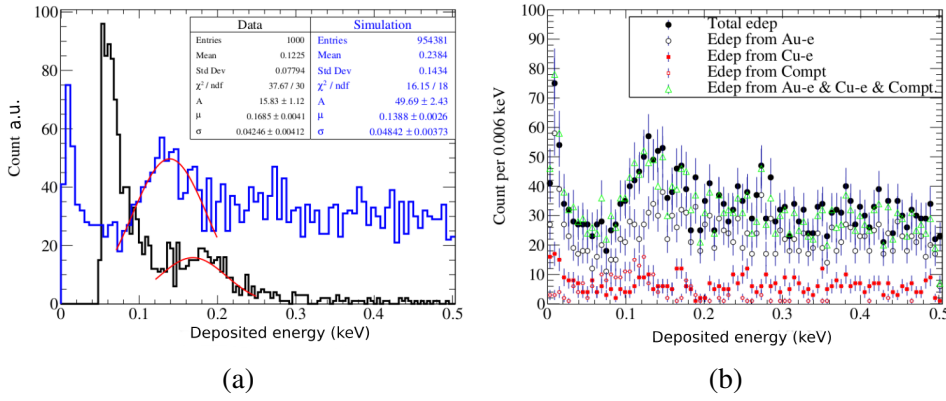
Figure 3: Simulated energy deposition in a sapphire (Al_2O_3) module, zoomed in the low energy region where a bump is observed. (a) the simulated spectrum in comparison to the measured spectrum. (b) the contributions of various sources to the bump extracted from the simulation.

found to be dominantly due to the gold layer around the source. The X-rays from the source interact with the gold layer producing electrons which end up in the sapphire target and create this bump. The contributions from various sources to the energy depositions in the "bump region" are shown in Fig. 3(b). Whether the bump in the measured spectrum is due to the same sources as found from simulation could not be finally decided for not having GEANT4 models validated at such a low energy. The ELOISE [6] project is actively looking into the sub-keV energy region to derive reliable models for accurate energy loss simulation in this regime. We intend to re-investigate this effect of source encapsulation when more accurate models are available in the future.

5. Conclusion

In this contribution, we discuss the CRESST background model and its recent extension, incorporating advanced fitting techniques, additional background components, and material screening as priors in the fits. The newly developed model demonstrates an improved ability to accurately replicate the observed continuous background in a $CaWO_4$ crystal module. We intend to extend the model further with an increasing knowledge of background sources, considering surface contamination on the crystal, and incorporating various choices of target materials, like Al_2O_3, Si, for CRESST-III detector. Future iterations will account for calibration sources such as ^{55}Fe, utilized in recent runs, within the background model. In this proceeding, we investigate the impact of this source on the energy deposition spectrum. Our findings reveal that the source's position relative to the bulk and wafer detectors in the silicon module influences the relative number of X-rays escaping from the respective detectors. Furthermore, the encapsulation around the source causes a suppression in the relative number of events between the K_α and K_β peaks in the silicon module, and produces a bump around 140 eV in the spectrum of the sapphire module. Simulation results align well with the measured spectrum in silicon; however, the bump in the sapphire spectrum appears at a lower energy than observed in the measurement. We plan to investigate this discrepancy further with the availability of accurate models at sub-keV energies, potentially from the ELOISE project, in the future.

6. Acknowledgments

References

[1] A.H. Abdelhameed, G. Angloher, P. Bauer, A. Bento, E. Bertoldo, R. Breier et al., *Geant4-based electromagnetic background model for the CRESST dark matter experiment*, *Eur. Phys. J. C* **79** (2019) 881 [1908.06755].

[2] G. Angloher, S. Banik, G. Benato, A. Bento, A. Bertolini, R. Breier et al., *Secular equilibrium assessment in a CaWO$_4$ target crystal from the dark matter experiment CRESST using Bayesian likelihood normalisation*, *Appl. Radiat. Isot.* **194** (2023) 110670 [2209.00461].

[3] G. Angloher, S. Banik, G. Benato, A. Bento, A. Bertolini, R. Breier et al., *High-dimensional bayesian likelihood normalisation for cresst's background model*, 2307.12991.

[4] A. Fuß, *Simulation based Neutron Background Studies for the CRESST and COSINUS Dark Matter Search Experiments*, Ph.D. thesis, Vienna, Tech. U., 2022. 10.34726/hss.2022.86617.

[5] G. Angloher, S. Banik, G. Benato, A. Bento, A. Bertolini, R. Breier et al., *Results on sub-GeV dark matter from a 10 eV threshold CRESST-III silicon detector*, *Phys. Rev. D* **107** (2023) 122003 [2212.12513].

[6] H. Kluck, *ELOISE - Reliable background simulation at sub-keV energies*, *SciPost Phys. Proc.* **12** (2023) 064 [2212.12634].
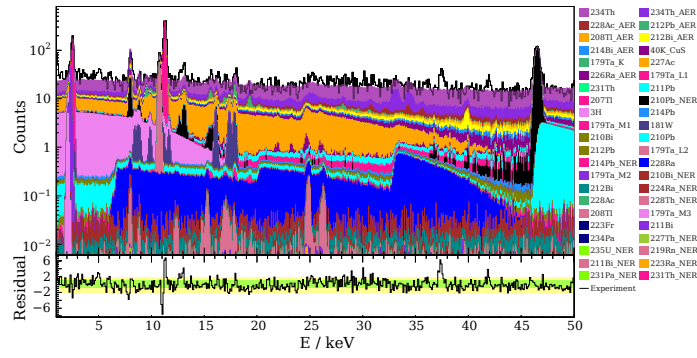
A. Appendix

Figure 4: Stacked templates from simulation in the ROI scaled to the reference data by Likelihood Normalization Method (LNM) [3].
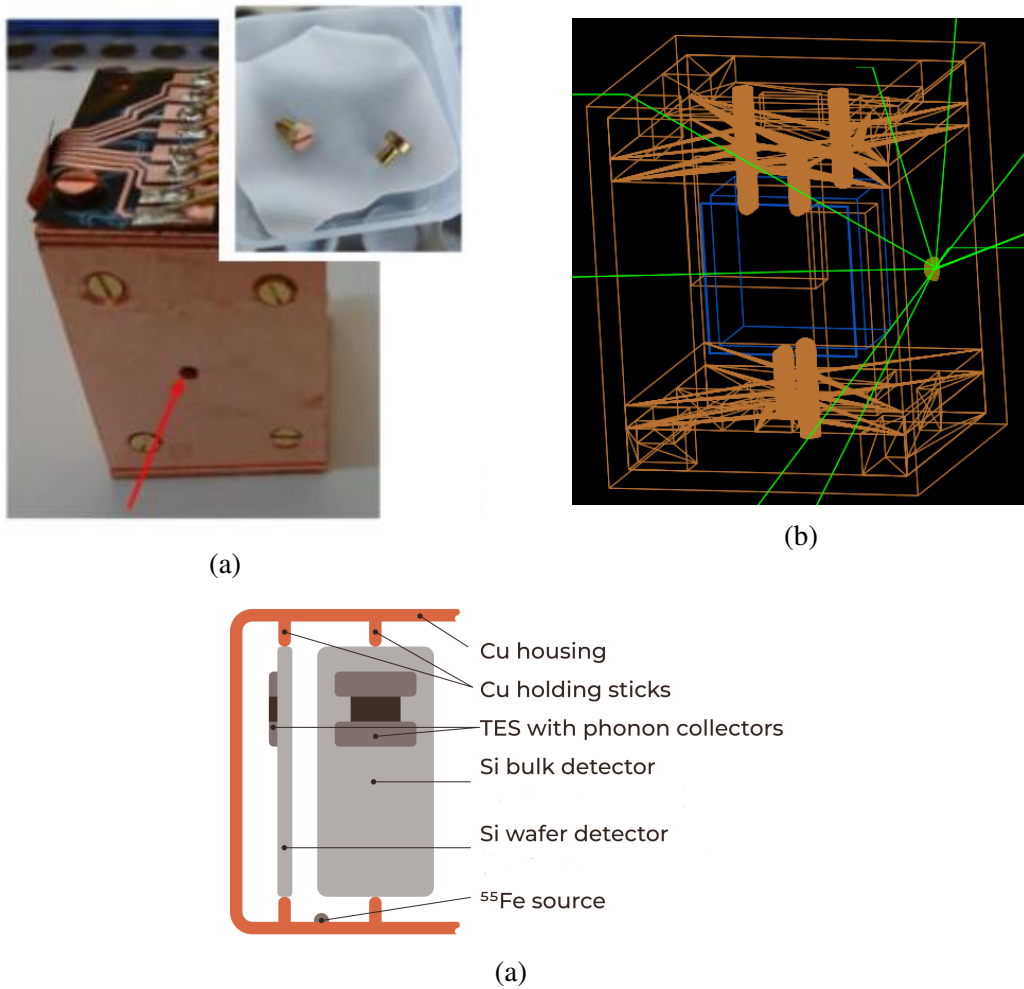

(a)

(b)

(a)

Figure 5: (a) A photo of the ^{55}Fe source (inset). The source is deposited on the end of a screw and then covered by layers of glue and gold. The red arrow indicates where the source will be screwed in the housing of a CRESST III module. (b) Visualization of the source and the detector module with ImpCRESST. (c) Schematic of the silicon module along with the ^{55}Fe source facing the bulk and wafer detectors assyemtrically in the module.